

*oncolytic virotherapy, feedback mechanism,  
crow search algorithm, Immune-LQR*

*Mohammed A. HUSSEIN\**, *Ekhlas H. KARAM\**, *Rokaia S. HABEEB\**

## **CANCER GROWTH TREATMENT USING IMMUNE LINEAR QUADRATIC REGULATOR BASED ON CROW SEARCH OPTIMIZATION ALGORITHM**

### **Abstract**

*The rapid and uncontrollable cell division that spreads to surrounding tissues medically termed as malignant neoplasm, cancer is one of the most common diseases worldwide. The need for effective cancer treatment arises due to the increase in the number of cases and the anticipation of higher levels in the coming years. Oncolytic virotherapy is a promising technique that has shown encouraging results in several cases. Mathematical models of virotherapy have been widely developed, and one such model is the interaction between tumor cells and oncolytic virus. In this paper an artificially optimized Immune-Linear Quadratic Regulator (LQR) is introduced to improve the outcome of oncolytic virotherapy. The control strategy has been evaluated in silico on number of subjects. The crow search algorithm is used to tune immune and LQR parameters. The study is conducted on two subjects, S1 and S3, with LQR and Immune-LQR. The experimental results reveal a decrease in the number of tumor cells and remain in the treatment area from day ten onwards, this indicates the robustness of treatment strategies that can achieve tumor reduction regardless of the uncertainty in the biological parameters.*

### **1. INTRODUCTION**

With more than 17 million cases registered in 2018 and reports indicating that this number will reach 23.6 million in 2030, cancer is one of the most common diseases around the world (Cancer Research UK, 2016; NIH, 2016). Cancer is the name given to a group of diseases that share a set of common characteristics, rapid uncontrollable cell division and spread into surrounding tissues (Jenner, 2020). The reason for this rapid and uncontrolled growth of cells is mutation in signaling that regulates the growth and division processes within the cells (Priya & Reyes, 2015). Conventional cancer treatment includes surgery, chemotherapy, radiotherapy, targeted therapy, immunotherapy and stem cell transfusion therapy (Cancer Research UK, 2016).

The effectiveness of cancer treatment has improved significantly in recent years, but despite this there are certain types of cancer for which treatment options are still limited,

---

\* Mustansiriyah University, College of Engineering, Computer Engineering Department, Baghdad, Iraq, mohammediyad95@gmail.com, ek\_karam@yahoo.com, rokaia.shalal@uomustansiriyah.edu.iq

and there are tumors that remain completely incurable, which increases the need for long-term treatment strategies (Crivelli et al., 2012).

Biotherapy is a cancer treatment that uses the ability of viruses to infect and replicate to destroy cancer cells, these viruses are often called oncolytic viruses (Arum, Handayani & Saragih, 2019). Viruses favorably act on cancer cells rather than healthy cells. There are many viruses that have proven effective against cancerous tumors, including them Adenovirus, Reovirus, Measles, Herpes Simplex, Vesicular-Stomatitis Virus (VSV) (Crivelli et al., 2012).

Oncolytic virotherapy has shown success in some patients although this is not clear how to obtain good results in all cases. It is difficult to set the injections' number, quantity and scheduling to reduce the tumor size within specified time frame (Anelone, Villa-Tamayo & Rivadeneira, 2020).

Mathematical modelling help in prediction of the system's future behavior and assess the impact of variables and parameters on the overall dynamics of a cancer. These parameters are relevant to the patient's physiology, treatment strategy and disease type. It is challenging, risky, and expensive to carry out such expectations in vivo, vitro, or clinical trials (Cancer Research UK, 2016). These models can be used to improve and optimize the impact of different factors such as changes in the virus's genetics, dosage, or injection schedule.

Optimization is the achievement of the desired goal (s) exactly or roughly by obtaining the best set of variables maybe by trial and error. Nature inspired optimization algorithms are metaheuristic algorithms developed from biological principles, swarm behavior, and chemical or physical processes (Yang, 2020). Crow search algorithm (CSA) an algorithm inspired by crow's behavior was introduced in (Askarzadeh, 2016), its main use in solving engineering problems that contain constraints.

Recently, many researches aim to apply biological information processing systems to engineering fields due to its flexibility. As these systems are more flexible than currently available systems, which makes it possible to form a system whose performance is better than the performance of conventional systems (Takahashi & Yamada, 1998). Regulation Mechanism of Bio-Inspired Systems like the immune system, is a complex system consisting of many types of immune cells and appropriate communication channels. This is an ideal control system for the human body against diseases and foreign bodies (Ding, Chen & Hao, 2018).

Interactions between virotherapy and control theory have been illustrated in many previous studies. For instance, reducing the number of cancer cells using successive state dependent algebraic Riccati equation (SDARE) have been introduced in (Arum, Handayani & Saragih, 2019). In (Saputra, Saragih & Handayani, 2019)  $H_\infty$  were used to control the controller input into a system, the results showed the effectiveness of the  $H_\infty$  controller in reducing the number of Human Immunodeficiency Virus (HIV) particles in the blood plasma; In (Anelone, Villa-Tamayo & Rivadeneira, 2020) impulsive controller is designed to deliver a personalized dose for each case, and feedback controller showed a tumor reduction potential better than that obtained by former protocols.

In this paper, the principle of the body's immune mechanism is presented as a controller with LQR based on CSA for parameters optimization are used to control the number of viruses given to patients. To accomplish these objectives, the result of personal protocol is investigated as a reference for comparison (Anelone, Villa-Tamayo & Rivadeneira, 2020).

The remaining sections of this paper are organized as follows, the mathematical model is discussed in the second part, the immune system is defined in the third part, and the crow

search algorithm (CSA) is demonstrated in the fourth part. The fifth section includes a definition of the proposed Immune-LQR structures controller. The simulation results and review of the proposed controllers are addressed in the sixth section, and the conclusion is presented in the final section.

## 2. MATHEMATICAL MODELLING

In the studies (Jenner et al., 2018; Kim et al., 2011), nude mice were given a genetically modified virus to reduce the number of breast cancer cells in it in just 60 days. Since these naked mice have no immune system, the tumor reduction is entirely due to the oncolytic virotherapy. Experiments began with mice containing between 90 and 300 cancer cells. All experiments follow a fixed protocol in injecting  $10^{10}$  viral particles on days 0, 2, 4. The interaction between oncolytic virus and carcinoma cells shown in Fig. 1, and illustrated mathematically using (ordinary differential equations) ODEs according to work in (Jenner et al., 2018):

$$\dot{S}(\tau) = r \log\left(\frac{K}{S(\tau)}\right) - \frac{\beta V(\tau)S(\tau)}{S(\tau) + I(\tau) + \varepsilon} \quad (1)$$

$$\dot{I}(\tau) = \frac{\beta V(\tau)S(\tau)}{S(\tau) + I(\tau) + \varepsilon} - d_I I(\tau) \quad (2)$$

$$\dot{V}(\tau) = Uv(\tau) - dvV(\tau) + \alpha d_I I(\tau) \quad (3)$$

where,  $\dot{S}$  denotes the density of susceptible tumor cells ( $\times 10^6$  cells),  $\tau$  represents the time,  $r$  is the tumor growth ( $\text{day}^{-1}$ ),  $K$  describes the carrying capacity ( $\text{cell} \times 10^6$ ),  $\beta$  is the tumor cells rate of infection ( $\text{day}^{-1}$ ),  $\dot{I}$  refers to the density of infected tumor cells ( $\times 10^6$  cells),  $d_I$  is the infected tumor cells death rate ( $\text{day}^{-1}$ ),  $\dot{V}$  is the density of virus particles ( $\times 10^9$  virus),  $dv$  is the viral decay ( $\text{day}^{-1}$ ) and  $\alpha$  viral burst size (virus  $\times 10^9$ ).

$T=S+I$  is the total number of tumor cells,  $\varepsilon$  is a small value ( $\varepsilon > 0$ ) set to avoid singularity occurring as  $(S+I)$  approaches zero.

The injection of virus particles is expressed by the model's input  $Uv(\tau)$ . While  $T$  represents the model's output. The tumor volume is calculated as  $T = 0.523 \times H \times B^2$ , where,  $(H)$  is the height and  $(B)$  is the breadth. Both  $(H)$  and  $(B)$  are measured with a caliper (Kim et al., 2011). Then, assuming a density of  $10^6$  cells per  $\text{mm}^3$ ,  $T$  is calculated (Jenner et al., 2018).

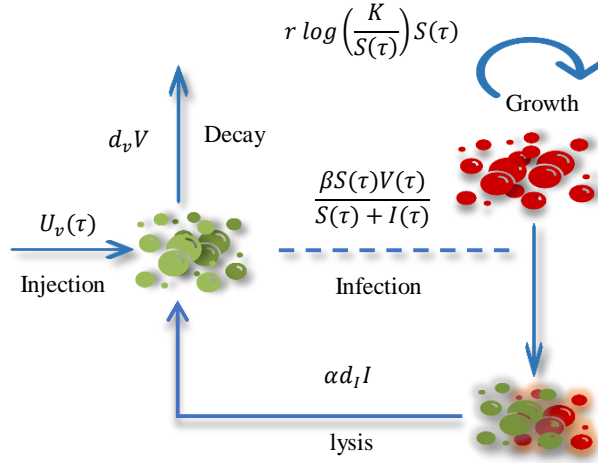


**Fig. 1. An interface between oncolytic viruses and tumor cells**

In Fig. 1, tumor cells are represented by red balls, while virus particles are represented by green balls). Table 1 summarizes the model's initial conditions and parameter values for AD- PEG-HER treatment.

**Tab. 1. Parameters and initial conditions values (Jenner et al., 2018)**

<i>Symbol</i>	$S_0$	$I_0$	$V_0$	$r$	$K$	$\beta$	$d_I$	$d_v$	$\alpha$
$S_1$	238.3535	0	0	0.0378	8466.8	1.12	2	2.0872	2
$S_2$	200.0340	0	0	0.0733	3179.1	1.4987	1.9995	3.2287	2.0015
$S_3$	101.5400	0	0	0.0224	4922.4	0.2	2	3.5	2
$S_4$	140.3436	0	0	0.0316	8317.1	1.2108	0.1	1.8730	3.7748
$S_5$	128.1481	0	0	0.0603	936.4293	1.3606	0.1	1.8416	3.7541
unit	Cells	cells	virus	day <sup>-1</sup>	cells $\times$ $10^6$	day <sup>-1</sup>	day <sup>-1</sup>	day <sup>-1</sup>	virus $\times$ $10^9$

### 3. IMMUNE FEEDBACK MECHANISM

Recent immunology researches have shown that the immune system is essential in protecting the body against complex and hostile changes in the environment through the interaction between antibodies and lymphocytes. Antigens have the potential to impact the immune system's simultaneous dynamics (Rochdi, 2014). This process is known as the immune T-cell regulatory circuit because of T cells' primary function in the immune response (Takahashi & Yamada, 1998).

The main cells in this process are  $Ab$  antibodies,  $Ag$  antigens,  $B$  cells, suppressor  $T$  cells  $T_s$  and  $T$  helper cells  $T_h$ . Antigen Information is passed on to  $T$  cells as antigens infect the body.

After receiving the message, the  $T$  cells activate the  $B$  cells, which then produce antibodies to remove the antigen. The number of  $T_h$  cells in the human body increases as the number of antigens increases, and more  $B$  cells can be produced to protect the body (Rochdi, 2014).

$T_s$  cells number in the body will increase and consequently  $B$  cells will decrease, in conjunction with the decrease in the antigen level. After a while the immune system begins to balance out. The immune system is able to react quickly to foreign bodies and regulate the immune system as a result of this collaboration between the feedback mechanism and the related mechanism (Rochdi, 2014). The suppression function of  $B$  cells will be discussed here.  $B$  cells are triggered and restricted by  $T_s$  cells in response to antigen invasion, so the  $B$  cells consistency of  $t^{th}$  cell generation can be determined by (Rochdi, 2014):

$$B(t) = T_H(t) - T_S(t) \quad (4)$$

$$T_H(t) = K_1 \alpha(t) \quad (5)$$

$$T_S(t) = K_2 \{f[\Delta B(t - d)]\} \alpha(t) \quad (6)$$

where  $B(t)$  represents the consistency of  $B$  cells,  $K_1$  and  $K_2$  represents the helper and suppressor genes respectively,  $\alpha(t)$  refers to the  $t^{th}$  generation antigen consistency,  $f$  is a nonlinear function, that represents the relationship between the antigen and antibody, that elicits from the  $B$  cells,  $d$  is the time delay of the immune response and  $\Delta B$  refers to the change of consistency in the  $B$  cell that can be determined by:

$$\Delta B(t - d) = B(t - d) - B(t - d - 1) \quad (7)$$

From equations (4–6), the relationship between the antigen and the  $B$ -cell's consistency, can be expressed as:

$$B(t) = K_1 \{1 - \eta_0 f[\Delta B(t - d)]\} \alpha(t) \quad (8)$$

where  $\eta_0$  is the proportional coefficient between  $T_H$  and  $T_S$ ,  $\eta_0 = K_2/K_1$ . The immune feedback mechanism performs two inconsistent processes simultaneously: it reacts quickly to foreign bodies and works to restore the immune system stability. Additionally, a high level of antibodies must be coordinated and controlled because they can be harmful to the body. Deviation must be avoided in a complex regulation control system to ensure system stability, which is consistent with the immune system's target.

#### 4. CROW SEARCH ALGORITHM

Crow search algorithm (CSA) is an optimization algorithm that mimics the crow flock behavior in storing and retrieving their surplus food (Askarzadeh, 2016).

Generally, the adjustable parameters of CSA are: population (flock) size ( $N$ ), Flight length ( $FL$ ), awareness probability ( $AP$ ) and maximum number of iterations ( $Maxiter$ ). The implementation of CSA can be done by the following steps:

1. Define the optimization problem and initialize the decision variables and any constraints needed.
2. The position and memory of each crow is initialized (each crow represents a viable solution to the optimization problem).
3. Evaluate the position of each crow using a fitness function.
4. Generate new position in the search space.
5. Determine the viability of new positions.
6. Evaluate the new position's fitness feature.
7. Update the crow memory by the new position.
8. Verify the termination criterion.

In this paper the CSA is used to tune the parameters of the Immune-LQR ( $k_1$  and  $\eta$ ,  $k_1$ ,  $k_2$ , and  $k_3$ ). The CSA can be described by the following flowchart:

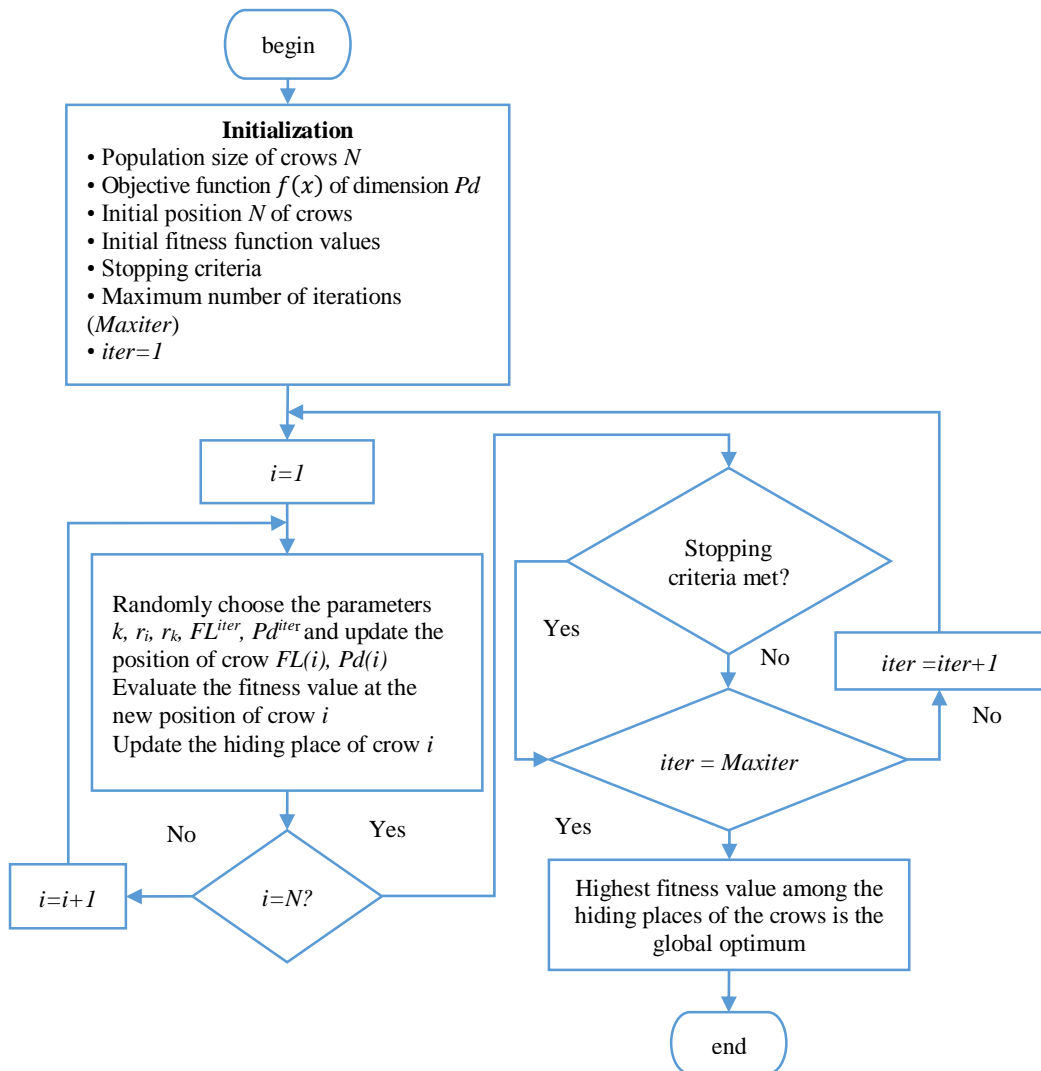


Fig. 2. CSA Flowchart

## 5. PROPOSED CONTROLLER

In this paper the continuous administration of viruses using an Immune-LQR controller are suggested to monitor the number viruses provided to patients. The CSA is used to tune immune and LQR parameters. The study is conducted on two subjects, S1 and S3, with LQR and Immune-LQR. The block diagram of the suggested controller is shown in Fig 3.

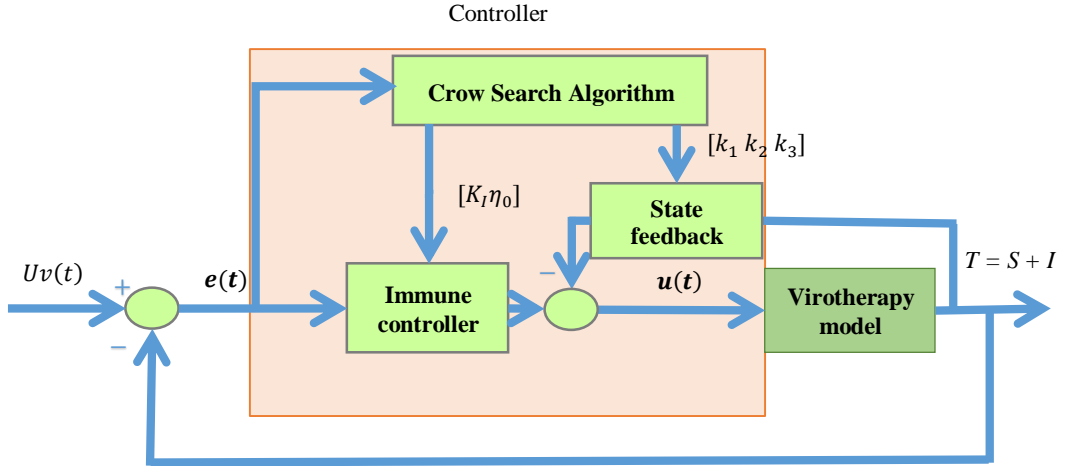


Fig. 3. Block diagram of the suggested Immune -LQR controller based on optimization algorithm

The error  $e(t)$  represents the amount of antigen ( $\alpha(t)$  in equation 8), and the controller's input  $u(t)$  will be the total incentive that the  $B$  cells accept. Then the feedback control system is defined as follows:

$$u(t) = u1(t) \times u2(t) \quad (9)$$

$$u1(t) = K_1 \{1 - \eta_0 f[\Delta u(t - d)]\} e(t) \quad (10)$$

$$u1(t) = K_I e(t)$$

where  $K_I$  is defined as the immune controller gain that is specified by the gene  $\eta_0 = K_2/K_1$ . The parameter  $K_1$  controls the response speed, the parameter  $\eta_0$  controls the stabilization effect and  $f(\cdot)$  denotes a nonlinear-function. This function is chosen as  $T$  cell's controls action-function, which is influenced by antigen consistency on antibody in immune response. The function  $f(x)$  is defined by:

$$f(x) = 1.0 - \exp\left(\frac{-x^2}{a}\right), \quad a > 0 \quad (11)$$

where  $a$  is a parameter that changes the function shape. the range of  $f(x)$  is  $[0,1]$ . The value of  $a$  determines the active region of  $x$ . The output of the immune controller can be described as:

$$u1(t) = K_1 \left\{ 1 - \eta_0 \left( 1.0 - \exp \left( \frac{-x^2}{a} \right) \right) \right\} e(t) \quad (12)$$

$$u1(t) = K_I e(t)$$

Since the immune controller is a nonlinear gain controller, it is not robust against noise and error induced by nonlinear disruption. To solve this problem and improve the system's efficiency, the immune controller must be combined with conventional LQR ( $\mathbf{u2}(t)$ ). LQR was chosen because it can handle large disturbances while maintaining system stability without reducing working efficiency and can handle previous disturbances (Purnawan & Purwanto, 2017). When the forward gain  $k_1$  of the LQR is multiplied by the immune output, the final result is  $\mathbf{K}_{I1}$ , as shown in Fig 3, and Eq. 23 shows the structure's controller output.

$$\dot{x} = Ax + Bu \quad (13)$$

$$y = Cx \quad (14)$$

$$u(t) = -kx + r \quad (15)$$

where  $\dot{x}$  denotes the state vector,  $u$  is referred to the control signal,  $y$  is the output and  $r$  represents the reference. The equations (1-3) can be written as a matrix as follows:

$$\begin{bmatrix} \dot{S} \\ \dot{I} \\ \dot{V} \end{bmatrix} = \begin{bmatrix} -r + r \ln \left( \frac{L}{S} \right) - \beta \frac{IV}{(I+S)^2} & \beta \frac{VS}{(I+S)^2} & -\beta \frac{S}{I+S} \\ \beta \frac{IV}{(I+S)^2} & -\beta \frac{IV}{(I+S)^2} - d_I & \beta \frac{S}{I+S} \\ 0 & \alpha d_I & -d_V \end{bmatrix} \begin{bmatrix} S \\ I \\ V \end{bmatrix} + \begin{bmatrix} 0 \\ 0 \\ 1 \end{bmatrix} Uv \quad (16)$$

$$y = [1 \ 1 \ 0] \begin{bmatrix} S \\ I \\ V \end{bmatrix} \quad (17)$$

The matrix  $A$  will differ based on the equilibrium point chosen, but the matrices  $B$  and  $C$  will remain the same (Anelone, Villa-Tamayo & Rivadeneira, 2020). Dynamic system in equations (13–15) can be written as:

$$\dot{x} = [A][x] + [B]u + [0]r \quad (19)$$

If  $x(\infty)$  and  $u(\infty)$  reach constant value, then  $y(\infty) = r$ , and the system is stabilized. The state and control signal error becomes as follow:

$$x(t) - x(\infty) = x_e(t)$$

$$u(t) - u(\infty) = u_e(t)$$

The state error equation can be written as:

$$x_e(t) = [A][x_e(t)] + [B]u_e(t) \quad (20)$$

with:

$$u_e(t) = -Kx_e(t) \quad (21)$$

$$e(t) = [x_e(t)]$$

$$u_2(t) = -Kx_e(t)$$

The LQR method is used to find the value of  $K$ , and the LQR cost function is defined by:

$$J = 1/2 \int_0^{\infty} (e^T Q e + u_e^T R u_e) dt \quad (22)$$

where  $Q$  is a positive-definite (or positive-semidefinite) Hermitian or real symmetric matrix,  $R$  is a positive-definite Hermitian or real symmetric matrix. and Ricarte's equation is:

$$A^T P + P A + Q - P B R^{-1} B^T P = 0 \quad (23)$$

where  $P$  is a positive-definite Hermitian or real symmetric matrix, with:

$$K = -[k_1 \ k_2 \ k_3]$$

From equation (9), (12) and (21):

$$u(t) = u_1(t) \times u_2(t)$$

$$u_1(t) = K_I e(t)$$

$$u_2(t) = -K x_e(t)$$

The first LQR gain ( $k_1$ ) is multiplied by immune gain ( $K_I$ ), then substituting equation (12) into equation (18) yields:

$$u(t) = -[K_I k_1 \ k_2 \ k_3] \quad (24)$$

$$K_{I1} = K_I k_1$$

$$u(t) = -[K_{I1} \ k_2 \ k_3]$$

where Eq. (23) represents control input.

## 6. SIMULATION RESULTS AND ANALYSIS

In this paper, toxicity and the subsequent dosages of viral injections was not considered as a limitation in the design of the controller. The toxicity tests in (Kim et al., 2011) revealed that when the oncolytic adenovirus's surface is shielded with a biocompatible polymer like polyethylene glycol (PEG), the virus therapy causes no hepatic damage and minimal liver toxicity.

For contrast, the same target in (Anelone, Villa-Tamayo & Rivadeneira, 2020) will be used, which states that the goal of the treatment is to reduce and sustain the total number of tumor cells below 50 cells in 60 days with discrete viral injections. The well-known PSO (partial swarm optimization algorithm) is used for comparison purpose with CSA. The Optimal control parameters obtained using optimization algorithms for  $S_1$  and  $S_3$  using LQR and Immune-LQR controller listed in Table 2 and 3 respectively (the  $a$ ,  $Q$  matrix, and  $R$  are

selected as:  $0.5, \begin{bmatrix} 0 & 0 & 0 \\ 0 & 0 & 0 \\ 0 & 0 & 1 \end{bmatrix}, [0.1]$ ).

**Tab. 2. Optimal parameters for LQR controller**

<i>Algorithms</i>	<i>k1</i>	<i>k2</i>	<i>k3</i>	<i>subjects</i>
CSA	-6.6522	5.1449	3.1093	} S1
PSO	-7.1520	2.1023	2.4930	
CSA	-27.9204	3.6500	6.7346	} S3
PSO	-27.9640	0.7472	1.4617	

**Tab. 3. Optimal parameters for Immune-LQR controller**

<i>Algorithms</i>	<i>k1</i>	<i>k2</i>	<i>k3</i>	$\eta_0$	$K_I$	<i>subjects</i>
CSA	-5.9762	2.5627	6.1470	0.2243	3.7401	} S1
PSO	-5.8598	2.4347	2.4930	0.6066	4.9352	
CSA	-25.1379	2.7631	7.2516	0.5570	3.8160	} S3
PSO	-27.9640	2.2416	1.4617	0	4	

The parameters used in optimization algorithms are listed in Table 4.

Tab. 4. Optimization algorithms parameters.

Parameters	Value	Algorithms
population size( $N$ )	25	} CSA, PSO
Max iteration ( $Maxiter$ )	50	
problem dimension ( $Pd$ )	5	} CSA
Awareness probability ( $AP$ )	1.2	
Flight length ( $FL$ )	0.3	
Inertia weight( $w_{max}-w_{min}$ )	(0.9 – 0.4)	} PSO
Learning rates ( $c1, c2$ )	2	

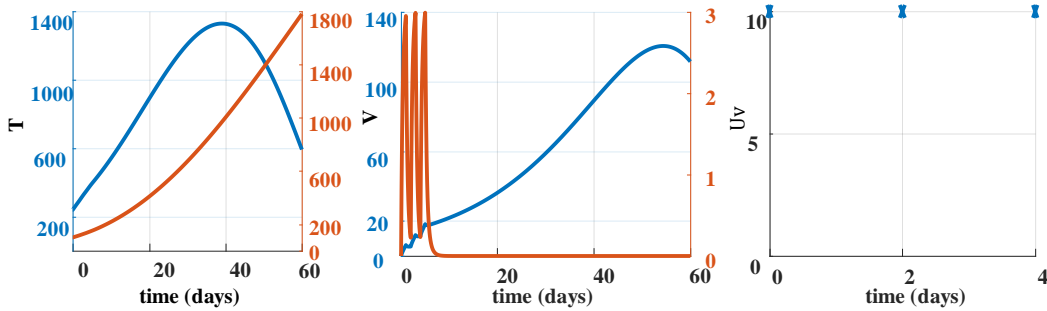
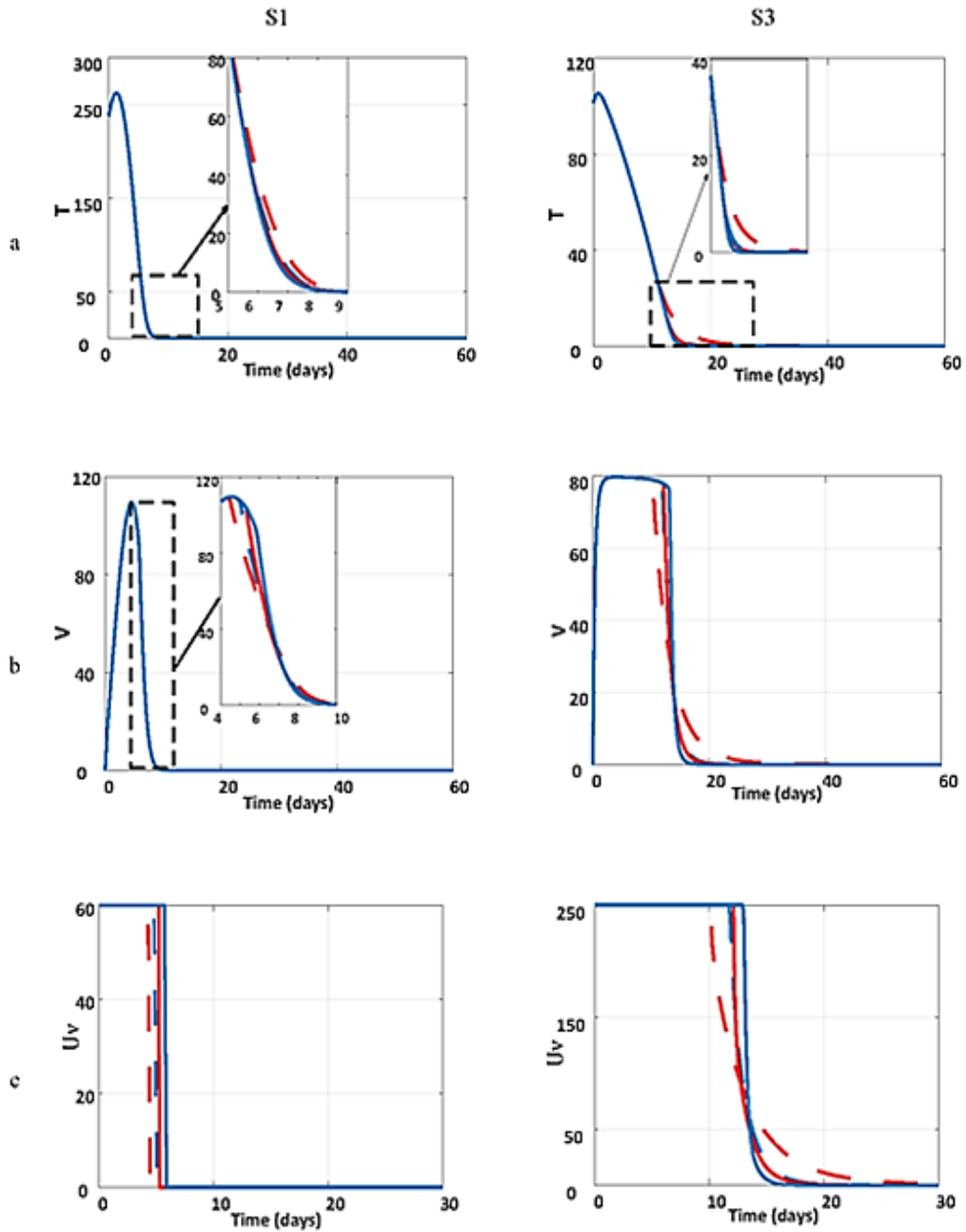


Fig. 4. Simulation result of experimental protocol for  $S_1$  (blue line) and  $S_3$  (orange line)

Fig 4. shows the experimental protocol results of  $S_1$  and  $S_3$ . The left figure illustrates the total number of tumor cells over a period of 60 days. The middle figure illustrates the viral loads in vivo over the period of 60 days. The right figure illustrates the viral injections within 4 days. This is the treatment of subject  $S_1$  and  $S_3$  with the total injections of 10.

As illustrated in Fig. 4, the experimental treatment fails to reduce the size of the tumor in  $S_1$  while the tumor begins to regress after an initial rise in  $S_3$ ; traditional therapy with different subjects has various effects.

In Fig. 5, the orange dash lines and the continuous lines indicate subjects with LQR and Immune-LQR controllers respectively optimized using the PSO algorithm for number of injections determination; while the blue dash lines and the continuous lines indicate subjects with LQR and Immune-LQR units respectively optimized using the CSA algorithm for number of injections determination. The top row (a) shows the total number of tumor cells within 60 days. The middle row (b) shows the viral loads in vivo within 60 days. The bottom row (c) shows the viral injections within 30 days.



**Fig. 5. Simulation result of S1(left column) and S3(right column) using Immune-LQR control and different optimization algorithms**

The feedback control reduces the size of the tumor faster than the conventional treatment, and there are no rebounds of the tumor after the end of the treatment, as the feedback controller works to keep the tumor with therapeutic zone, i.e., less than or equal to 50 total tumour cells in all subjects, and reduce the amount of injections overtime as showing in Fig.

5(a). The personalized protocol suggested using the proposed control would give higher initial injections than the experimental treatment. Consequently, the feedback mechanism in the immune controller increases the number of injections due to an increase in the  $\eta_0$ , where the larger ratio indicates the increase of  $T_h$  cells whose increase leads the body to form more antibodies to protect itself as shown in Fig. 5(b). As a result, the control signal is higher in treatment with feedback control than in experimental treatment during the first hours of treatment and decreases gradually as shown in Fig. 5(c). Nevertheless, the virus load tends to be lower in the feedback control compared to the experimental treatment. After the tumor has decreased in recent days, we suggest that viruses that may be toxic are quickly removed.

The results suggest applying control theory in oncolytic virotherapy has benefits by delivering an effective amount of treatment to accomplish therapeutic goals, as both LQR and Immune-LQR controllers perform this task in a relatively shorter period with superior performance Immune-LQR over LQR at S1 by 3.1807%, 1.4020% and at S3 by 2.5490%, 2.2083% using CSA and PSO respectively where the performance index used is Integral time absolute error (ITAE). Since each subject has different biological rate, they react differently across different elements. When tumor regression is as slow as in S3, the total injection will increase, implying that there is a negative relationship between the total number of injections and the tumor regression speed to overcome high starting spikes.

The results obtained are consistent with (Anelone Villa-Tamayo & Rivadeneira, 2020), as a high injection in the beginning performs well through different subjects and reduces the total number of tumor cells and total injections. When significant amounts of viral loads are injected at the start of therapy in any subject, the total number of tumor cells and the total doses are reduced. However, increased viral loads in vivo and the eventual expensive cost of viral injections pose questions about toxicity in this case. The tumor decreases and remains in the treatment area from day ten onwards; This indicates that the controller regulates the number of injections well to reduce the tumor.

## 7. CONCLUSION

In this paper, artificially tuned Immune-LQR controller is suggested to regulate the number of viral load injections that are injected in order to reduce tumor cells. The mathematical model of interaction between tumor cells and oncolytic virotherapy has been considered. In order to improve the characteristics of the proposed controllers, CSA and PSO algorithms has been applied. The simulation results show that the Immune-LQR structure outperforms the other structures. As the feedback controller acts to maintain the tumor within the therapeutic region, i.e., less than or equal to 50 total tumor cells in all subjects, and minimize the amount of injections over time, the feedback control decreases the size of the tumor faster than traditional therapy, and there are no rebounds of the tumor after the treatment ends.

To improve our understanding of the relationship between toxicity, number of viral injection doses, and viral load in vivo, further mathematical and experimental research is required. These findings may help with the development of virus therapies and control strategies to ensure tumour regression with minimal side effects.

## REFERENCES

- Anelone, A.J.N., Villa-Tamayo, M.F., & Rivadeneira, P.S. (2020). Oncolytic virus therapy benefits from control theory. *Royal Society Open Science*, 7(7), 200473. <https://doi.org/10.1098/rsos.200473>
- Arum, A.K., Handayani, D., & Saragih, R. (2019). Robust control design for virotherapy model using successive method. *Journal of Physics: Conference Series*, 1245(1), 12054. <https://doi.org/10.1088/1742-6596/1245/1/012054>
- Askarzadeh, A. (2016). A novel metaheuristic method for solving constrained engineering optimization problems: crow search algorithm. *Computers & Structures*, 169, 1–12. <https://doi.org/10.1016/j.compstruc.2016.03.001>
- Cancer Research UK. (2016). *Worldwide cancer statistics*. Cancer Research UK. Cancer Research UK (pp. 1–5). <https://www.cancerresearchuk.org/health-professional/cancer-statistics/worldwide-cancer>
- Crivelli, J.J., Földes, J., Kim, P.S., & Wares, J.R. (2012). A mathematical model for cell cycle-specific cancer virotherapy. *Journal of Biological Dynamics*, 6(sup1), 104–120. <https://doi.org/10.1080/17513758.2011.613486>
- Ding, Y., Chen, L., & Hao, K. (2018). *Bio-Inspired Collaborative Intelligent Control and Optimization*. Springer.
- Jenner, A.L. (2020). Applications of mathematical modelling in oncolytic virotherapy and immunotherapy. *Bulletin of the Australian Mathematical Society*, 101(3), 522–524. <https://doi.org/10.1017/S0004972720000283>
- Jenner, A.L., Yun, C.-O., Kim, P.S., & Coster, A.C.F. (2018). Mathematical modelling of the interaction between cancer cells and an oncolytic virus: insights into the effects of treatment protocols. *Bulletin of Mathematical Biology*, 80(6), 1615–1629. <https://doi.org/10.1007/s11538-018-0424-4>
- Kim, P.-H., Sohn, J.-H., Choi, J.-W., Jung, Y., Kim, S.W., Haam, S., & Yun, C.-O. (2011). Active targeting and safety profile of PEG-modified adenovirus conjugated with herceptin. *Biomaterials*, 32(9), 2314–2326. <https://doi.org/10.1016/j.biomaterials.2010.10.031>
- NIH. (2016). *Cancer Statistics – National Cancer Institute*. NIH. <https://www.cancer.gov/about-cancer/understanding/statistics>
- Priya, P., & Reyes, V.M. (2015). *A Cancer Biotherapy Resource*. ArXiv Preprint ArXiv:1602.08111. <https://arxiv.org/abs/1602.08111>
- Purnawan, H., & Purwanto, E.B. (2017). Design of linear quadratic regulator (LQR) control system for flight stability of LSU-05. *Journal of Physics: Conference Series*, 890(1), 12056.
- Rochdi, B. (2014). Design and application of fuzzy immune PID control based on genetic optimization. *International Workshop on Advanced Control IWAC* (pp. 10–14).
- Saputra, J., Saragih, R., & Handayani, D. (2019). Robust  $H_\infty$  controller for bilinear system to minimize HIV concentration in blood plasma. *Journal of Physics: Conference Series*, 1245(1), 12055.
- Takahashi, K., & Yamada, T. (1998). Application of an immune feedback mechanism to control systems. *JSME International Journal Series C Mechanical Systems, Machine Elements and Manufacturing*, 41(2), 184–191. <https://doi.org/10.1299/jsmec.41.184>
- Yang, X.-S. (2020). *Nature-inspired optimization algorithms*. Academic Press.